Neutron Compton scattering

1996 J. Phys.: Condens. Matter 8 5955

(http://iopscience.iop.org/0953-8984/8/33/005)

J. Phys.: Condens. Matter **8** (1996) 5955–5975. Printed in the UK

REVIEW ARTICLE

Neutron Compton scattering

G I Watson

Rutherford Appleton Laboratory, Didcot, Oxfordshire OX11 0QX, UK

Received 22 May 1996

Abstract. Neutron Compton scattering measurements have the potential to provide direct information about atomic momentum distributions and adiabatic energy surfaces in condensed matter. First applied to measuring the condensate fraction in superfluid helium, the technique has recently been extended to study a variety of classical and quantum liquids and solids. This article reviews the theoretical background for the interpretation of neutron Compton scattering, with emphasis on studies of solids.

1. Introduction

Neutron Compton scattering is set apart from other branches of neutron scattering by the magnitude of energy and momentum transfers involved, typically in excess of 1 eV and 30 $Å^{-1}$, respectively. Neutron scattering is renowned as a sensitive probe of collective properties in condensed matter, but in this extreme range of energies and momenta—the impulse limit—it is single-particle properties that are probed. The scattering occurs so rapidly, compared with the time-scales of atomic motion in the sample, that the measured response is rather simply related to the equilibrium momentum distribution of the atoms.

Thus, the term neutron Compton scattering refers, not to a distinct type of scattering, but to the usual neutron scattering cross-section in a limiting range of parameters. In the impulse limit, the scattered intensity, as a function of energy for fixed momentum transfer $\boldsymbol{Q}$, consists of a peak centred at $E_R = \hbar^2 Q^2/2M$, the energy of recoil of a stationary nucleus on colliding with a neutron. The dependence of the peak position on the mass M of the struck atom implies that the scattering from different atoms appears at different energies. This ability to separate contributions from different atomic species (and isotopes) is a useful feature of the technique.

Doppler broadening results in a recoil peak whose width is proportional to the mean kinetic energy of the atoms, and whose detailed shape depends on the distribution of atomic momenta. The principal tool in interpreting experiments is the impulse approximation, which predicts a precise relationship between the scattering data, in the form of the Compton profile, and the atomic momentum distribution. This gives an opportunity to compare results of experiments with predictions of realistic theoretical models of microscopic properties.

As the name suggests, neutron Compton scattering is closely related to experimental techniques in other branches of physics [1]. Compton scattering [2–4], i.e. inelastic scattering of x-rays, gamma rays or (10–60 keV) electrons provides information on electron momentum distributions, an example being the direct observation of the Fermi–Dirac distribution for conduction electrons in metals. In nuclear physics, an established technique for probing the momentum distribution of nucleons in nuclei is deep inelastic scattering

0953-8984/96/335955+21$19.50

[5, 6] of protons or electrons with energies of 100–1000 MeV and de Broglie wavelengths of the order of nuclear radii. At still higher energies (10 GeV and above), deep inelastic scattering of electrons, muons or neutrinos [7–9] probes the internal structure of nucleons and has been a key experiment in the confirmation of the existence of quarks. By analogy with these techniques, neutron Compton scattering is sometimes called deep inelastic neutron scattering.

Neutron Compton scattering was first suggested [10] as a technique for measuring of the condensate fraction in superfluid ^{4}He, and this has been an active field for three decades (see [1, 11, 12] and references therein). Recently, the development of spallation neutron sources, which have much higher intensities than reactor sources in the incident energy range required for neutron Compton scattering, have opened up new applications. Recent experiments include studies of condensed noble gases [13–16], metals [17, 18], normal liquid ^{4}He [16, 19–21], liquid ^{3}He [22], solid ^{4}He [21], superfluid ^{3}He–^{4}He mixtures [23], and molecular hydrogen and deuterium [24–27].

The extreme momentum transfers now experimentally reachable imply that, in some cases, the corrections to the impulse approximation are essentially negligible. This suggests the possibility of direct and model-independent extraction of momentum distributions from Compton profiles, in contrast to the usual approach of fitting theoretical predictions to the experimental profiles. Though its feasibility has not yet been demonstrated in practice, this approach, if successful, could establish neutron Compton scattering as the only technique capable of measuring atomic momentum distributions directly. A particularly interesting case is where the motion of the atom of interest is well described by an effective (Born–Oppenheimer) potential, or adiabatic energy surface. An example is a proton bound in a heavy lattice. In this case, the momentum distribution is the squared amplitude of the Fourier transform of the proton wave function, and from it, the potential energy function can be extracted [28, 29].

The information obtainable in neutron Compton scattering is to some extent complementary to that from diffraction experiments. The former measures the Fourier transform of a *time-averaged* density; the latter the *instantaneous* momentum density. Thus, for example, a neutron Compton scattering experiment on protons in a double-well potential of a hydrogen bond [28, 29] could, in principle, distinguish between a wave function with amplitude in both wells, and a statistical mixture of states in which the proton is localized in one well or the other.

This article aims to summarize the theoretical framework for the interpretation of neutron Compton scattering experiments, with an emphasis on applications to solids. A thorough discussion of the physical principles underlying the impulse approximation is given in section 2, based on the central concept of the scattering time. Section 3 addresses the problem of extracting information from the Compton profile. In the final section we discuss briefly the potential of the direct inversion approach. Although some examples are drawn from published experimental studies, no attempt is made here to review current experimental activity. For further background material, see [30, 31].

2. The impulse approximation

We begin with an expression for the quantity which is measured in experiments, namely the partial differential cross-section for the scattering of a beam of neutrons by a collection of atomic nuclei. Although the nucleon–nucleon interaction is very strong, it is sufficiently short-ranged that the scattering is a weak perturbation of the incident wave. Therefore, with the aid of a Fermi pseudopotential, the scattering may be described in the first Born

approximation, and as a consequence the cross-section depends only on the changes in energy and wave vector of the neutron. We shall denote these by

$$\hbar\omega = \frac{\hbar^2}{2m}(k^2 - k'^2) \qquad \text{and} \qquad \boldsymbol{Q} = \boldsymbol{k} - \boldsymbol{k}' \tag{1}$$

respectively, where $\boldsymbol{k}$ and $\boldsymbol{k}'$ are the incident and scattered neutron wave vectors. A second simplifying assumption appropriate in the case of neutron Compton scattering is that the spatial scale of the scattering event, set by $1/Q$, is too small for one to detect correlations between the positions of different nuclei, and hence that the scattering may be described to a good approximation as incoherent. This approximation is particularly good for scattering from protons, where the incoherent cross-section is larger than the coherent cross-section by almost two orders of magnitude. Under these circumstances the contribution to the scattering cross-section from nuclei of a particular species is proportional to the response function [32]

$$S_i(\boldsymbol{Q}, \omega) = \frac{1}{2\pi\hbar}\int_{-\infty}^{\infty} \mathrm{d}t\, \mathrm{e}^{-\mathrm{i}\omega t} \sum_j Y_j(\boldsymbol{Q}, t) \tag{2}$$

where

$$Y_j(\boldsymbol{Q}, t) = \langle \mathrm{e}^{-\mathrm{i}\boldsymbol{Q}\cdot\boldsymbol{R}_j} \mathrm{e}^{\mathrm{i}\boldsymbol{Q}\cdot\boldsymbol{R}_j(t)} \rangle \tag{3}$$

is the density–density correlation function corresponding to the nucleus of atom j, whose position is represented by the quantum mechanical operator $\boldsymbol{R}_j$. The corresponding $\boldsymbol{R}_j(t)$ has a time dependence in the Heisenberg representation of

$$\boldsymbol{R}_j(t) = \mathrm{e}^{\mathrm{i}Ht/\hbar}\boldsymbol{R}_j\mathrm{e}^{-\mathrm{i}Ht/\hbar}. \tag{4}$$

The angular brackets in equation (3) denote a thermal average of the enclosed expression, as well as an implicit average over degrees of freedom which are passive in the scattering process, such as nuclear spin and neutron polarization states.

The physical content of the response function can be made more transparent by passing to a somewhat less general expression. The thermal average in equation (3) involves, in principle, a sum over expectation values with respect to the complete set of stationary quantum states of the many-body Hamiltonian describing the nuclei and other particles, and their interactions. Let us suppose that the motion of a particular nucleus can be represented by an effective single-particle Hamiltonian which describes its interaction with its environment, and a corresponding set of single-particle states. We have in mind the case of a nucleus bound in a molecule, where an effective potential is constructed using the Born–Oppenheimer scheme. Let us denote the effective single-particle states by $|n\rangle$ and their energies by E_n. The contribution to the response function from a single nucleus reduces to

$$S_i(\boldsymbol{Q}, \omega) = \sum_{nn'} Z^{-1}\mathrm{e}^{-E_n/k_BT}\,|\langle n|\mathrm{e}^{-\mathrm{i}\boldsymbol{Q}\cdot\boldsymbol{R}}|n'\rangle|^2\delta(\hbar\omega - (E_{n'} - E_n)) \tag{5}$$

where Z is a normalization factor (the thermodynamic partition function). In this expression we may recognize a sum over transitions from initial states n, weighted by a thermal Boltzmann factor, to final states n', of a transition probability. The latter is given by Fermi's golden rule as the product of a squared matrix element and an energy-conserving delta function. The scattering is represented by the operator $\mathrm{e}^{-\mathrm{i}\boldsymbol{Q}\cdot\boldsymbol{R}}$ which couples the plane wave of the neutron with the position of the nucleus.

Returning now to the general expression, equation (2), the form of the response function as a sum of separate contributions from each nucleus reflects the nature of the

incoherent approximation, which neglects correlations between different nuclei. The impulse approximation, which is the main topic of this section, consists in a similar neglect of *time* correlations in the motion. To be specific, if the time-scale of the scattering event is much shorter than the characteristic time of atomic motions in the sample, then the nuclei may be regarded as free particles in so far as the scattering probability is concerned. As a result, the latter depends only on the momentum of the nucleus in its initial state. Crudely speaking, then, we may summarize the approximations appropriate for neutron Compton scattering as follows: the Born approximation, that each neutron scatters only once; the incoherent approximation, that each scattering process involves only one nucleus; and the impulse approximation, that the neutron remains in the vicinity of the nucleus for a time too short to sense anything except how fast the nucleus is moving. This last approximation is the most subtle of the three, and it will be discussed in detail now.

2.1. The short-time expansion

Motivated by the idea that only short times are relevant, let us suppose that the correlation function $Y(\boldsymbol{Q}, t)$ for a single nucleus is dominated by its behaviour for small t. The time-dependent Heisenberg operator $\boldsymbol{R}(t)$ has the Taylor expansion

$$\boldsymbol{R}(t) = \boldsymbol{R} + (\boldsymbol{P}/M)t + \tfrac{1}{2}(\boldsymbol{F}/M)t^2 + \cdots \tag{6}$$

where $\boldsymbol{P} = M\dot{\boldsymbol{R}} = \mathrm{i}M[H, \boldsymbol{R}]/\hbar$ is the momentum of the struck nucleus which has mass M, and $\boldsymbol{F}$ is the force defined similarly. All of the operators in the expansion are evaluated at $t = 0$. We remark that the identification of $M\dot{\boldsymbol{R}}$ with momentum is valid only in the absence of velocity-dependent forces, i.e. it is assumed that there are no magnetic fields present, and that the motion of the nucleus is non-relativistic.

Reserving for later the question of the precise criteria for validity of the present mathematical procedure, let us examine the form of the response function resulting from the neglect of terms of order t^2 and higher. This amounts to an assumption that the struck particle is effectively free so that $\boldsymbol{F} = 0$. With the aid of the operator identity

$$\mathrm{e}^{A+B} = \mathrm{e}^{A}\mathrm{e}^{B}\mathrm{e}^{-(1/2)[A,B]} \tag{7}$$

which holds when $[A, B]$ commutes with both A and B, the correlation function is found to reduce to

$$Y(\boldsymbol{Q}, t) = \langle \mathrm{e}^{\mathrm{i}(\boldsymbol{Q}\cdot\boldsymbol{P}/M + \omega_R)t} \rangle \tag{8}$$

where $\omega_R = \hbar Q^2/2M$ is the (free-atom) recoil frequency. The exponent has an interpretation in terms of the kinematics of a neutron–nucleus collision. If the momentum of the nucleus is $\boldsymbol{P}$ before the collision, then it is $\boldsymbol{P} + \hbar\boldsymbol{Q}$ after the collision, and energy conservation requires

$$\omega = [(\boldsymbol{P} + \hbar\boldsymbol{Q})^2 - P^2]/2M\hbar = \boldsymbol{Q}\cdot\boldsymbol{P}/M + \omega_R. \tag{9}$$

In particular, $\hbar\omega_R$ is the energy imparted to a stationary nucleus by a collision with a neutron.

If the nucleus were indeed at rest before the scattering, equation (8) would give $Y(\boldsymbol{Q}, t) = \mathrm{e}^{\mathrm{i}\omega_R t}$, and the response function would consist of a delta-function line at the recoil frequency. In fact, the nucleus will be in a quantum state having a distribution of initial momenta, and the line will therefore be Doppler broadened. Each possible initial momentum results in a contribution to the scattering intensity at a frequency given by the conservation constraint, equation (9). Specifically, defining the momentum distribution by

$$n(\boldsymbol{q}) = \langle \delta(\boldsymbol{q} - \boldsymbol{P}/\hbar) \rangle \tag{10}$$

the response function in the impulse approximation is

$$S_i(\boldsymbol{Q},\omega) = \bar{h}^{-1}\int n(\boldsymbol{q})\delta(\omega - \bar{h}\boldsymbol{Q}\cdot\boldsymbol{q}/M - \omega_R)\,\mathrm{d}\boldsymbol{q}. \tag{11}$$

This result, that the scattering cross-section is directly related to the momentum distribution of the struck nuclei, is of central importance in neutron Compton scattering experiments.

It is important to emphasize that, although it represents a single-particle response, the momentum distribution $n(\boldsymbol{q})$ is actually a property of the many-body system of all of the nuclei and their interactions. In other words, the momentum distribution of a single nucleus depends on its environment and therefore on the behaviour of the system as a whole. Let us examine again the special case where the motion of a nucleus is given by a set of effective single-particle states $|n\rangle$. Here, equation (10) becomes

$$n(\boldsymbol{q}) = (1/2\pi)^3 \sum_n Z^{-1}\mathrm{e}^{-E_n/k_BT}\left|\int \mathrm{e}^{-\mathrm{i}\boldsymbol{q}\cdot\boldsymbol{r}}\langle\boldsymbol{r}|n\rangle\,\mathrm{d}\boldsymbol{r}\right|^2. \tag{12}$$

At zero temperature, this reduces to the square modulus of the Fourier transform of the ground-state wave function. Thus, there is a direct relationship between the measured quantity, $S_i(\boldsymbol{Q},\omega)$, and the quantum mechanical wave functions of the nuclei in the sample.

2.2. The scattering time

Looking at the short-time expansion of the nucleus's position operator, equation (6), we see that the first term neglected in the derivation of the impulse approximation is proportional to the operator $\boldsymbol{F}$ representing the force experienced by the nucleus. Denoting root mean square values by an overbar, the corrections are expected to be small if

$$\overline{\boldsymbol{F}\cdot\boldsymbol{Q}}\,\tau_s \ll \overline{\boldsymbol{P}\cdot\boldsymbol{Q}} \tag{13}$$

where τ_s is a quantity with the dimensions of time, identified as the time-scale of the scattering process, or *scattering time*. At first sight, it might appear reasonable to relate τ_s to the time taken for a neutron wave packet to pass the vicinity of the nucleus. The corollary, that the degree of coherence of the neutron beam plays a role in deciding the validity of the impulse approximation, is largely erroneous, as will be demonstrated presently.

To establish the significance of the scattering time, let us adopt the operational point of view that, since the aim is to approximate the correlation function $Y(\boldsymbol{Q},t)$, the relevant time-scale should be obtained from $Y(\boldsymbol{Q},t)$ itself. The response function $S_i(\boldsymbol{Q},\omega)$, as we have seen, consists in general of a peak centred at the recoil frequency ω_R, with a certain width $\Delta\omega$. It follows that the general form of $Y(\boldsymbol{Q},t)$ is of an oscillatory function $\mathrm{e}^{\mathrm{i}\omega_R t}$, modulated by a decreasing envelope of width $1/\Delta\omega$ (figure 1). The fact that $Y(\boldsymbol{Q},t)$ goes to zero confirms our expectation from physical arguments that knowledge of the struck atom's motion for a limited time span is sufficient to predict the scattering response. Accordingly, we identify the scattering time τ_s as the time-scale for the decay of the correlation function $Y(\boldsymbol{Q},t)$ to zero, which equals $1/\Delta\omega$, the reciprocal of the recoil peak width [12]. If it happens that $S_i(\boldsymbol{Q},\omega)$ is highly structured, i.e. has features on several frequency scales, this means that $Y(\boldsymbol{Q},t)$ depends on more than one characteristic time. The overall decay envelope is determined by the longest of these characteristic times, and it follows that τ_s is the reciprocal of the width of the *narrowest* feature in $S_i(\boldsymbol{Q},\omega)$.

Strictly speaking, for scattering from solids the correlation function $Y(\boldsymbol{Q},t)$ does not go to zero, but to $|\langle\mathrm{e}^{\mathrm{i}\boldsymbol{Q}\cdot\boldsymbol{R}}\rangle|^2$, corresponding to the amplitude of the elastic line in $S_i(\boldsymbol{Q},\omega)$ [32]. However, this constant component does not affect the argument: since we are interested

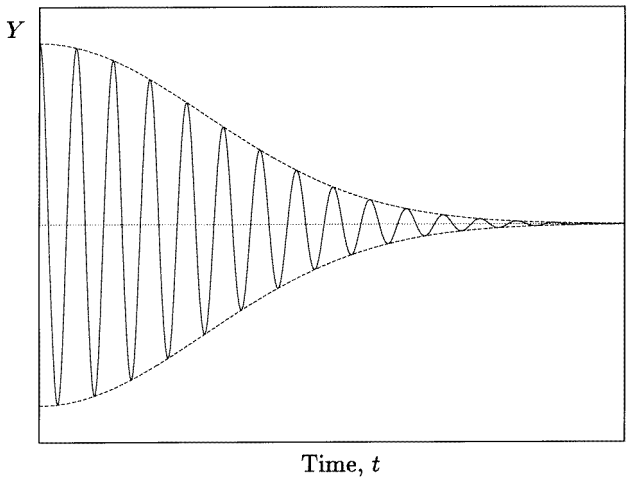

Figure 1. The schematic form of the correlation function $Y(\boldsymbol{Q}, t)$, whose Fourier transform is proportional to the neutron scattering cross-section. The frequency of the oscillations is the reciprocal of the recoil frequency of the scatterer, and the amplitude falls off on a scale of the scattering time τ_s.

in the scattering at energies near $\omega = \omega_R$, we may discard the elastic scattering and take $Y(\boldsymbol{Q}, t)$ to consist only of the inelastic part, which tends to zero as described.

With τ_s defined in terms of the structure of the response function, a rigorous determination requires, in principle, a detailed calculation of $S_i(\boldsymbol{Q}, \omega)$ for the system of interest. In the absence of a detailed theory, some rough estimates can be made. A convenient procedure is to estimate τ_s self-consistently using the impulse approximation itself. We take for $S_i(\boldsymbol{Q}, \omega)$ a peak centred on ω_R of width $\Delta\omega$. According to equation (11), $\Delta\omega$ is proportional to the width of the distribution of P_Q, the projection of momentum $\boldsymbol{P}$ along the direction of $\boldsymbol{Q}$, and thus

$$\tau_s \sim \frac{M}{Q\langle P_Q^2\rangle^{1/2}}. \tag{14}$$

The inverse dependence of the scattering time on Q is an essential feature. It implies that, as anticipated on physical grounds, the impulse approximation becomes exact in the limit of large wave-vector transfer. This statement is true provided that the forces on the nuclei are always finite, for if $\boldsymbol{F}$ can grow arbitrarily large the condition in equation (13) is not satisfied no matter how short the scattering time. We shall therefore not consider pathological cases, such as scattering from a 'hard-core' fluid [33] or from a particle undergoing Brownian motion [34], where corrections to the impulse approximation do not become negligible as $Q \to \infty$.

With our estimate, equation (14), for the scattering time, the criterion for validity of the impulse approximation reads

$$\overline{F_Q}(1/Q) \ll \langle P_Q^2\rangle/M \tag{15}$$

where $F_Q = \boldsymbol{F} \cdot \boldsymbol{Q}/Q$ is the projection of the force onto the direction of $\boldsymbol{Q}$. This has the following interpretation. If $1/Q$ is regarded as the length scale of the scattering event, it is required that the work done by the force F_Q in moving the nucleus this distance be negligible compared with the root mean square kinetic energy of the nucleus due to

motion along $\boldsymbol{Q}$; in other words, forces on the nucleus do not change its energy appreciably during the scattering process. This feature of impulsive scattering is reflected in the energy-conserving delta function in equation (11), which would otherwise involve a contribution from the nucleus's change in potential energy.

An alternative discussion of the short-time expansion can be made within the framework of the Gaussian approximation for incoherent scattering [35], in which the correlation function is written as $Y(\boldsymbol{Q}, t) = \exp[-Q^2 w(t)]$, with the width function $w(t)$ proportional to the mean square displacement of the atom at time t. The impulse approximation is obtained in an asymptotic analysis by expansion of $w(t)$ about a saddle point in the complex plane. The correction terms may be estimated in terms of the moments of $S_i(\boldsymbol{Q}, \omega)$, and are small if the 'skewness' of the recoil peak, related to the third moment, is small. The condition for validity of the impulse approximation obtained in this way is equivalent to equation (15).

2.3. Bound nuclei

The preceding derivation of the conditions for validity of the impulse approximation is not rigorous, in that the use of the impulse approximation to predict its own range of validity is a circular argument. An example in which the reasoning fails is that of scattering from a nucleus bound in a harmonic potential. This example will now be treated in some detail. It will lead us to extend somewhat the concept of scattering time, and will serve as an introduction to a general discussion of scattering from nuclei bound in solids.

For the harmonic oscillator, $S_i(\boldsymbol{Q}, \omega)$ can be calculated without approximation [32]. It will be sufficient for our purposes to examine the case of zero temperature, for which the exact result is

$$S_i(\boldsymbol{Q}, \omega) = \hbar^{-1} \mathrm{e}^{-\omega_R/\omega_0} \sum_{n=0}^{\infty} [(\omega_R/\omega_0)^n / n!]\, \delta(\omega - n\omega_0). \tag{16}$$

The prediction of the impulse approximation is

$$S_i^{\mathrm{IA}} = (2\pi\hbar^2 \omega_0 \omega_R)^{-1/2} \exp\left[-\frac{(\omega - \omega_R)^2}{2\omega_0\omega_R}\right] \tag{17}$$

and the self-consistent estimate of its range of validity, from equation (15), is $\omega_R \gg \omega_0$. The two functions are compared in figure 2 for $\omega_R/\omega_0 = 15$. The exact $S_i(\boldsymbol{Q}, \omega)$ is an array of infinitely sharp lines, whereas the impulse approximation result is a smooth Gaussian, drawn as a dashed curve. The impulse approximation fails spectacularly to reproduce the fine structure of the spectrum.

As is evident from the general expression, equation (5), for the response function in terms of single-particle states, the source of the problem is energy quantization. Each sharp line represents the absorption of a number of quanta by the oscillator. Since $S_i(\boldsymbol{Q}, \omega)$ contains infinitely narrow structure, the scattering time, as defined above, is infinite, and the short-time expansion fails.

Not all is lost, however. Evidently, the impulse approximation does give an accurate account of the *envelope* of the palisade of delta functions. The agreement improves on increasing Q. In other words, the impulse approximation describes $S_i(\boldsymbol{Q}, \omega)$ on a frequency scale large compared with ω_0. In practice, such a coarse description is likely to be adequate. For nuclei bound in molecules or solids, even if broadening mechanisms intrinsic to the system (discussed below) are insufficient to smear out structure on a scale of ω_0, achieving the instrumental resolution needed to discern the separate lines would most likely be a difficult task, with an incident energy large enough to accomplish the experiment.

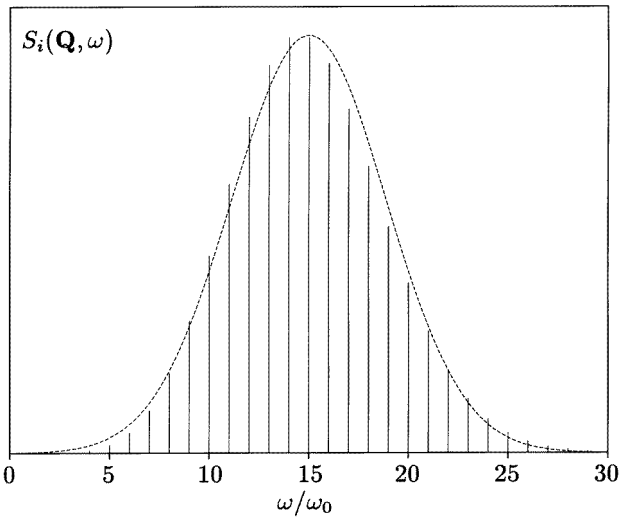

Figure 2. Solid vertical lines: the response function for scattering from a nucleus bound in an ideal harmonic well of frequency ω_0 (each delta-function contribution is plotted as a vertical line of height equal to the corresponding weight). The momentum transfer $\boldsymbol{Q}$ is such that the recoil frequency ω_R is $15\omega_0$. Dashed curve: the same quantity as predicted by the impulse approximation.

The ability of the impulse approximation to describe the envelope of the discrete spectrum is not restricted to the ideal oscillator. The generalization to arbitrary potential wells is straightforward [36]. At zero temperature, equation (5) is

$$S_i(\boldsymbol{Q},\omega) = \sum_n |\langle 0|\mathrm{e}^{-\mathrm{i}\boldsymbol{Q}\cdot\boldsymbol{R}}|n\rangle|^2 \delta(\hbar\omega - (E_n - E_0)). \tag{18}$$

The scattering intensity is concentrated at values of $\omega = (E_n - E_0)/\hbar$ for which the matrix element is large. Now, the essence of the impulse approximation is that the momentum transfer, and hence the energy transfer, is so large that the nucleus's final state is approximately that of a free particle, a plane wave. Substituting a final state $\mathrm{e}^{\mathrm{i}\boldsymbol{q}'\cdot\boldsymbol{R}}$ with $E_n = \hbar^2 q'^2/2M$ into equation (18) yields [37]

$$S_i(\boldsymbol{Q},\omega) = \int n(\boldsymbol{q})\delta[\hbar\omega - \hbar^2(\boldsymbol{Q}+\boldsymbol{q})^2/2M + E_0]\,\mathrm{d}\boldsymbol{q} \tag{19}$$

where $n(\boldsymbol{q})$ is the momentum distribution defined previously in equation (12). For each $\boldsymbol{q}$ there is a contribution to $S_i(\boldsymbol{Q},\omega)$ at a position relative to the recoil frequency

$$\omega - \omega_R = \hbar\boldsymbol{Q}\cdot\boldsymbol{q}/M + \hbar q^2/2M - E_0/\hbar. \tag{20}$$

For sufficiently large Q, the first term dominates the others on the right-hand side, and hence equation (19) is essentially identical to the impulse approximation derived using the short-time expansion.

In this re-derivation of the impulse approximation, three approximations were made. The first was the replacement of the final state by a plane wave in the evaluation of the matrix element in equation (18). Clearly it is sufficient that this approximation be accurate in the region of space where the ground-state wave function is appreciable, near the centre of the potential well. That this is indeed the case follows from the ideas of the WKB

approximation [38], in which the wave function of a bound state is written as a standing wave with a local wave vector $q'(x) = [2M(E_n - V(x))/\hbar^2]^{1/2}$. The impulse limit requires

$$V(x) \ll E_n \tag{21}$$

within the spatial extent of the ground state, since then $q'(x)$ is approximately independent of position. In addition, to ensure that the WKB wave function is a reasonable approximation of the excited state we require the fractional change in $q'(x)$ over one wavelength $2\pi/q'$ to be small [38]. In the present context this requires $\mathrm{d}V/\mathrm{d}x \ll q'E_n$, which is a weaker constraint than equation (21).

The second approximation made in re-deriving the impulse approximation was ignoring the discreteness of the spectrum of final states. That is, the sum in equation (18) was replaced by an integral over all momenta. It is here that the delta-function structure of $S_i(\boldsymbol{Q}, \omega)$ is lost, and the procedure is therefore justified if our aim is to calculate the envelope of the spectrum.

The final approximation was the neglect of the second and third terms of equation (20). Since $E_0 - \hbar^2 q^2/2M$ is, on average, the potential energy in the ground state, we obtain the condition

$$\langle V \rangle \ll \hbar Q \langle P_Q^2 \rangle^{1/2}/M. \tag{22}$$

This is evidently a stronger condition than equation (21) since the right-hand side increases only linearly with Q. Hence, if equation (22) is satisfied, all of the approximations leading to the impulse approximation are justified.

The condition may be expressed in terms of the forces on the atom by noting that $\boldsymbol{F} = -\boldsymbol{\nabla} V$. If $\bar{F}$ represents the root mean square force in the ground state, which has a spatial extent of order $\hbar/\langle P^2 \rangle^{1/2}$, then the ground-state potential energy is approximately $\hbar \bar{F}/\langle P^2 \rangle^{1/2}$. Inserting this estimate in equation (22) and ignoring any dependence on the direction of $\boldsymbol{Q}$ yields $\bar{F} \ll Q\langle P^2 \rangle/M$, in agreement with the self-consistent estimate, equation (15).

We conclude that the short-time expansion, and the associated self-consistent assessment of its validity, are adequate for scattering from a bound nucleus, provided that we are satisfied with a description of the envelope of $S_i(\boldsymbol{Q}, \omega)$. In this context, it is appropriate to define the scattering time τ_s as the inverse width of the narrowest envelope, which is the time-scale of processes during scattering which determine the broad structure of the response function.

The present discussion has considered atoms bound in potentials with infinitely high walls. In practice, of course, a sufficiently large impulse will eject the atom from the molecule or lattice which binds it. It has been suggested in the literature that the impulse approximation is valid only when the recoil energy is large compared with the binding energy E_B. This is indeed the condition necessary for the scattering response to be a smooth function as the impulse approximation predicts, rather than an array of narrow lines. However, the conclusion of this section is that there is an intermediate energy range, $\omega_0 \ll \omega_R < E_B/\hbar$, in which the impulse approximation provides an accurate description of the envelope of the response function.

2.4. Solids

We turn now to the subject of scattering from nuclei bound in a lattice, in which motions of different nuclei are coupled. In other words, we wish to generalize the preceding discussion, which treated lattice vibrations as a collection of independent oscillators (i.e. in an Einstein

model), to a situation where the vibrational modes are collective in nature. We aim to provide qualitative estimates for the range of Q for which the impulse approximation is an accurate description of the response function. The task of applying the impulse approximation in detailed calculations for particular model systems will not be attempted here; see, for example [32] and [39].

The first point to be made is that the picture of $S_i(\boldsymbol{Q}, \omega)$ as an array of delta-function lines is no longer appropriate when atomic vibrations are coupled. The reason is simply that final states excited by the scattering are drawn from a continuous distribution, namely the phonon density of states, rather than from a set of quantized levels as for the oscillator. To be specific, let us consider a perfect harmonic lattice, at zero temperature. Referring to equation (18), the final states are now taken to be excited states of the lattice as a whole, rather than single-particle states. It is convenient to group together terms with a given number of phonons excited. The leading term, then, has $\omega = 0$ and yields a delta-function elastic line just as for the harmonic oscillator. The one-phonon contribution, however, is not a sharp line but a continuous distribution proportional to the phonon density of states $Z(\omega)$. Explicitly [32, 39],

$$S_i(\boldsymbol{Q}, \omega) = \mathrm{e}^{-2W(Q)} \{\delta(\omega) + (\omega_R/\omega)Z(\omega) + \cdots\} \tag{23}$$

where $\mathrm{e}^{-2W(Q)}$ is the Debye–Waller factor. Continuing the series, the two-phonon term is the product of a matrix element $\mathrm{e}^{-2W}(\omega_R/\omega)^2$ and the two-phonon density of states:

$$\int_0^\infty Z(\omega')Z(\omega - \omega')\ \mathrm{d}\omega' \tag{24}$$

which is the convolution of Z with itself. Higher terms in the phonon expansion are proportional to repeated self-convolutions of Z, and therefore become progressively broader and smoother. If Q is large, by the time energy transfers of the order of the recoil energy are reached, the number of phonons excited is so large that the central limit theorem applies and the n-phonon density of states is essentially Gaussian. The different contributions merge to form a smooth recoil peak. These features are illustrated in calculations by Mayers, Andreani and Baciocco [40] using a Debye model, and by Evans *et al.* [41] and Fielding *et al* [42] using realistic densities of states for ZrH_2 and ZrD_2.

The smoothing effect of the continuous distribution of phonon states is a 'de-phasing' effect, i.e. $Y(\boldsymbol{Q}, t)$ decays because the spread in frequencies causes a loss of coherence over time. This is to be contrasted with decay of correlations due to damping mechanisms. The latter are a consequence of interactions of phonons with impurities, with electrons, and with each other (due to anharmonicity), resulting in a finite phonon lifetime. Such effects may be included in equation (18) by replacing the delta function by a peak of width equal to the inverse phonon lifetime.

The effects of finite temperature are to broaden the scattering response still further. They enter through both de-phasing and damping mechanisms: the former because of the k_BT spread in initial energies, the latter because the phonon lifetime is a decreasing function of temperature.

Let us summarize the various energy scales that have arisen in our discussion so far. The characteristic frequency of the phonons is the Debye frequency ω_D, corresponding to an energy scale typically of the order of a few hundred kelvin. For low temperatures, $k_BT \ll \hbar\omega_D$, the mean kinetic energy per atom, E_K, is of order $3\hbar\omega_D/4$, while for high temperatures it approaches the classical value $3k_BT/2$. The lifetime τ of phonons is related to the thermal conductivity of the solid by $K = Cv^2/3\tau$, where C is the heat capacity and v is the sound velocity [43]. Inserting representative values leads to an estimate that

the lifetime broadening $\hbar/\tau$ is typically 1 K or less, and hence negligible in comparison to other energy scales in the system.

The energy scales related to the scattering process are the recoil energy $\hbar\omega_R$, typically in excess of 1 eV, and the width $\Delta\omega$ of the recoil peak. These are the scales which determine the applicability of the impulse approximation. In view of the smoothing effect of the continuous phonon density of states, we judge that the self-consistent criterion for the validity of the impulse approximation is appropriate. In order to apply it, we require an estimate of the forces on an atom. For a harmonic oscillator, the mean square of one Cartesian component of the force is $M^2\omega_0^4\langle x^2\rangle = 2M\omega_0^2 E_K/3$, and thus for a harmonic or nearly harmonic solid F_Q is of the order of $(M\omega_D^2 E_K)^{1/2}$. The criterion for validity of the impulse approximation becomes

$$Q \gg (M\omega_D^2/E_K)^{1/2} \sim (M\omega_D/\hbar)^{1/2} \tag{25}$$

where the second estimate is valid for temperatures low compared with the Debye temperature. The quantity on the right is the inverse of the root mean square displacement of a harmonic oscillator of frequency $\omega_D/2$. Thus, the criterion for the impulse approximation is more easily satisfied if the atoms are weakly bound, as one would expect. As remarked previously [28, 40], Debye frequencies do not depend strongly on atomic mass, and hence the Q-value required to reach the impulse limit should increase with mass as $M^{1/2}$.

Neutron Compton scattering investigations of monatomic solids reported recently include experiments on argon, krypton and xenon [13, 14], lithium [17], sodium [18] and ^{4}He [21]. To take a representative example, lithium [17] has a mass of 7 a.m.u. and a Debye temperature of approximately 400 K, yielding the criterion $Q \gg 8$ Å^{-1} for the impulse limit. For $Q \sim 100$ Å^{-1}, the highest used in the experiment cited, the recoil frequency $\omega_R \sim 3$ eV, and the recoil peak width $\Delta\omega$ is about 0.3 eV.

These considerations are readily generalized to more complicated systems. An example is the hydrogen molecule, which has been the subject of recent experiments [24–27]. In this system the binding of protons within an H_2 molecule is much stronger than the forces between molecules. The mismatch of energy scales is reflected in the spectrum of vibrational states, which is envisaged as consisting of two bands: a broad acoustic band, corresponding to molecular motions characterized by the Debye frequency ω_D, and a narrow high-frequency band centred at the intramolecular vibrational frequency ω_V. The width of the narrow band is of the order of ω_D^2/ω_V. In H_2, ω_V is nearly two orders of magnitude greater than ω_D, and the molecular and intramolecular motions are effectively decoupled. The characteristics of the scattering are thus dominated by the intramolecular vibrations, and in fact Mayers [24] found the scattering from liquid H_2 to be indistinguishable from that from the polycrystalline solid. In the low-temperature limit ($k_B T \ll \hbar\omega_V$) appropriate here, the criterion for validity of the impulse approximation is $Q \gg (M\omega_V/\hbar)^{1/2} \sim 10$ Å^{-1}, well within the experimental range.

Similar arguments apply for scattering from light atoms in a heavy lattice [44], such as the proton in $KHCO_3$ [45]. Here the proton vibrational modes are found in a high-frequency band, narrower than the acoustic band by approximately $(M_1/M_2)^{1/2}$, and are effectively decoupled from other motions because of the large mass ratio.

2.5. Liquids

The case of scattering from liquids is the most well developed and, at the same time, the most controversial, application of the impulse approximation. Here we restrict ourselves to a few general remarks; details may be found elsewhere [10, 11, 47–57].

For a monatomic classical liquid, such as a condensed heavy noble gas [13], the application of the impulse approximation appears straightforward. For example, taking order-of-magnitude values for the force between atoms in the liquid near its triple point, $\langle F^2 \rangle^{1/2} \sim 10^3$ K Å^{-1} [13], and the kinetic energy $E_K = 3k_BT/2$ in the range 200 to 400 K, we obtain an estimate $Q \gg 5$ Å^{-1} for the impulse limit to be reached. Indeed, in the experiments cited, deviations from the impulse approximation were observed to be small at momentum transfers between 17 and 29 Å^{-1}.

The situation appears to be not very different for most monatomic quantum fluids, except, of course, that the evaluation of the kinetic energy must take account of the quantum zero-point motion of the atoms. Examples of recent experiments on normal liquids in which quantum effects are important include studies of ^{4}He [16, 19–21], ^{3}He [22] and neon [15, 16].

One way to estimate orders of magnitude is to use a 'cell model' of the liquid, in which, on short time-scales, an atom is assumed to move in a roughly spherical cage created by neighbouring atoms, with intermolecular potentials of, say, Lennard-Jones form. For example, Andreani *et al* [20] have argued that such a model, with the total interatomic potential represented by an effective harmonic vibrational frequency $\omega_0 = 14$ K, accounts reasonably well for the observed temperature dependence of the mean kinetic energy of normal liquid ^{4}He.

Assuming that the same model suffices to estimate the forces on an atom, we find that $Q \gg (M\omega_0/\hbar)^{1/2} \sim 1$ Å^{-1} is the condition for the impulse approximation to be accurate. In fact, this type of estimate is highly misleading. The impression that the impulse limit is attained for rather low Q results from the low mass and the fact that the attractive part of the Lennard-Jones potential is very weakly binding. However, the experience gained from a variety of theoretical and experimental investigations over the past few decades (see [11] and references therein) has shown that the repulsive 'hard-core'-like part of the interatomic potential is crucial in determining the validity of the impulse approximation. Indeed, as mentioned previously, for a true hard-core fluid the impulse limit is not reached no matter how large the momentum transfer [33].

For the most extreme example of a quantum liquid, ^{4}He in its normal and superfluid phases, the work of Silver [54–56] is a definitive theoretical study of corrections to the impulse approximation. Its conclusion is that, although the correction terms in a formal expansion of $S_i(\boldsymbol{Q}, \omega)$ as $\boldsymbol{Q} \to \infty$ are proportional to powers of $1/Q$ [49], the nearly hard-core nature of the interactions results in a broad range of crossover to the asymptotic limit, in which the corrections scale as $\log Q$. As a result, the corrections are not negligible, even for the highest Q-values that might conceivably be attained in experiments. Silver's work also provides a systematic method of calculating the corrections, which has been applied successfully in measurements of the condensate fraction in superfluid helium [57].

For non-monatomic liquids, there are complicating (and interesting) features arising from the internal structure of the molecule. Recent work includes experiments on molecular hydrogen and deuterium [24–27].

2.6. Corrections to the impulse approximation

Deviations of the response function $S_i(\boldsymbol{Q}, \omega)$ from the prediction of the impulse approximation are often collectively termed 'final-state effects', since they result from deviations of the final state of the scattering process from plane-wave form. In fact, since $S_i(\boldsymbol{Q}, \omega)$ reflects properties of initial as well as final states, and deviations arise from both sources [37, 40], we shall refer simply to 'corrections to the impulse approximation'.

In general, the corrections take the form of a broadening of the response function; this is in part an effect of a finite lifetime of the final state, due to collisions of the struck atom with its neighbours [10]. An example is the broadening effect of the phonon lifetime discussed in section 2.4. The corrections are frequently embodied in a 'final-state resolution function', which is convolved with the result of the impulse approximation to obtain the predicted Compton profile.

When deviations from the impulse approximation are appreciable, accurate calculations of the final-state resolution function require a detailed theory of interactions in the system under study. An example is the hard-core perturbation theory [50–52] for normal and superfluid ^{4}He, which is a quantum many-body theory of the fluid incorporating scattering data for the helium interatomic potential. Here, we shall not enter into details of such calculations, but make a few general comments, principally aimed at the case of scattering from solids for which the corrections are small.

Let us recall the approach taken in section 2.3 and [36], where the impulse approximation was derived under three assumptions: that the final state is nearly a plane wave, that the discreteness of the final-state energies is unimportant, and that the last two terms in the energy conservation condition, equation (20), may be neglected. The last assumption, that

$$E_0 \approx \hbar^2 q^2/2M \tag{26}$$

is exactly true only for a free-particle system. Mayers [37] has termed the deviations from equation (26) 'initial-state effects'. Here we focus on the fact that, as mentioned previously, equation (26) is the strongest of the three approximations made, and therefore if we relax it, the result is likely to be a better approximation than the impulse approximation. For example, if the final-state energy E_n is set equal to its WKB estimate $\hbar^2 q^2/2M + V(x)$, and if $E_0 - V(x)$ is replaced with its average value, namely the mean kinetic energy E_K, one obtains

$$S_i(\boldsymbol{Q}, \omega) = \int n(\boldsymbol{q})\delta[\hbar\omega - \hbar^2(\boldsymbol{Q} + \boldsymbol{q})^2/2M + E_K]\, \mathrm{d}\boldsymbol{q} \tag{27}$$

which is a result first suggested by Stringari [58]. It is a better approximation than the impulse approximation at low temperatures, but becomes less useful at higher temperature, since the replacement of a distribution of energies by an average ceases to be valid [40].

The Stringari formula shows that one aspect of the corrections to the impulse approximation is a shift of the maximum of the recoil peak to lower frequency. Such a shift is indeed visible in figure 2, for example. In addition, the corrections induce an asymmetry in the peak. This suggests that a straightforward symmetrization of the data can be used to remove partially deviations from the impulse approximation. In the Sears [49] method, symmetrization is the first step in a systematic self-consistent correction procedure. The method is based on a formal asymptotic expansion of $S_i(\boldsymbol{Q}, \omega)$ in powers of $1/Q$, in terms of successive moments of the final-state resolution function. It is found that symmetrization of the measured recoil peak eliminates corrections of order Q^{-1}, leaving residual terms of order Q^{-2}. The antisymmetric part of $S_i(\boldsymbol{Q}, \omega)$ is proportional to Q^{-1} and amounts to a measurement of deviations from the impulse approximation; this information can then be used to correct for the residual deviations in the symmetrized data, and the result is a response function corrected up to order Q^{-2}. Comparisons of correction methods for experimental data on bound light atoms have been made by Evans *et al* [41] and by Fielding *et al* [42].

An analysis method recently developed by Glyde [59], also based on moment expansions, aims to extract both the limiting impulse approximation response function, and measurements of the finite-Q corrections, from experimental neutron Compton scattering

data. In this approach, rather than concentrating on extreme momentum transfers in order to minimize deviations from the impulse approximation, one collects data over a broad range of Q. It is the measurable difference in the Q-dependence of various contributions to the expansion moments that allows the $Q \to \infty$ (impulse approximation) component of the data to be isolated, and the corrections to be estimated. This technique has been applied in a recent study of normal liquid ^{4}He and liquid neon [16].

3. The Compton profile

In this section we turn to the problem of extracting information about the momentum distribution from measured data. We shall take the approach [28, 29] of assuming that the impulse approximation is accurate. As we have seen, this assumption is justified in the case of scattering from solids, where the impulse limit is well within the experimental range of momentum transfers and where leading-order 'final-state' corrections can be handled, for example, by symmetrization of the data.

The measured response function $S_i(\boldsymbol{Q}, \omega)$ is given in the impulse approximation by equation (11). Let us define $J = (\hbar^2 Q/M)S_i$ and rearrange the delta function to give

$$J = \int n(\boldsymbol{q})\delta(\boldsymbol{q} \cdot \hat{\boldsymbol{Q}} - y)\ \mathrm{d}\boldsymbol{q} \tag{28}$$

where $\hat{\boldsymbol{Q}}$ is the unit vector along $\boldsymbol{Q}$, and

$$y = (M/\hbar Q)(\omega - \omega_R). \tag{29}$$

This form of $S_i(\boldsymbol{Q}, \omega)$ has an important consequence. Consider an isotropic system, where the scattering is independent of the direction of $\boldsymbol{Q}$. Then J depends only on the variable y, rather than on $\boldsymbol{Q}$ and ω independently. In other words, the data 'collapse' onto a function $J(y)$ of a single variable. This phenomenon is known as y-scaling, and $J(y)$ is termed the Compton profile. It is seen from the delta function in equation (28) that y is the projection of the atom's momentum onto the scattering vector.

The function $J(y)$ is a convenient and standard form for experimental results to be presented in. The recoil peak is shifted to be centred at $y = 0$, and if the profile is normalized to unity the mean kinetic energy per atom is directly related to the second moment of the Compton profile by

$$E_K = (3\hbar/2M)\int_{-\infty}^{\infty} y^2 J(y)\ \mathrm{d}y. \tag{30}$$

This result follows from the general moment relations for the incoherent response function [32].

For an anisotropic system such as a single crystal, the response function depends on the direction of $\boldsymbol{Q}$ as well as on y, and one then speaks of the directional Compton profile, $J(\hat{\boldsymbol{Q}}, y)$. It has a second moment related to the kinetic energy associated with motion along $\hat{\boldsymbol{Q}}$.

3.1. Reconstructing momentum distributions

The Compton profile and the momentum distribution are related by equation (28). Consider $J(\hat{\boldsymbol{Q}}, y)$ as a function of y for fixed $\hat{\boldsymbol{Q}}$, and define a coordinate system xyz such that $\hat{\boldsymbol{Q}}$ points along the z-axis. Then

$$J(\hat{\boldsymbol{Q}}, y) = \int n(q_x, q_y, y)\ \mathrm{d}q_x\ \mathrm{d}q_y. \tag{31}$$

The Compton profile is seen here to be the integral of $n(\boldsymbol{q})$ over a plane normal to the vector $\hat{\boldsymbol{Q}}$, i.e. a projection of the momentum density onto the direction of the momentum transfer. This mathematical relationship between $J(\hat{\boldsymbol{Q}}, y)$ and $n(\boldsymbol{q})$ is known as a Radon transform [60]. An important property of the transform is that it is invertible: given the directional Compton profile for all values of its arguments, the momentum distribution can be extracted.

The Radon inversion formula can be expressed in many mathematically equivalent forms, but these are not equivalent in practice, when the data are finite and affected by noise and instrumental resolution. The reconstruction problem for the Radon transform, and the associated mathematical questions of stability, uniqueness, accuracy and resolution, have been studied thoroughly in connection with computerized tomography in diagnostic radiology [61]. We note, in passing, that the Radon transform can be expressed in the framework of wavelet theory [62], but the consequences, if any, for the reconstruction problem do not appear to have been explored. Here we describe a reconstruction method proposed by Reiter (see [28, 29]) based on the work of Davison and Grunbaum [63, 64], which is a variant of the 'filtered back-projection' technique in common use in medical applications of tomography.

The method involves decomposing the angular ($\hat{\boldsymbol{Q}}$-) dependence of the data into spherical harmonics, and the y-dependence into products of Gaussian and Hermite functions. Specifically,

$$J(\hat{\boldsymbol{Q}}, y) = \pi^{-1/2} \mathrm{e}^{-(y/y_0)^2} \sum_{nlm} A_{nlm} H_{2n+l}(y/y_0) Y_{lm}(\hat{\boldsymbol{Q}}) \tag{32}$$

where Y_{lm} are the usual spherical harmonics, as defined, for example, in [38]. The constant y_0 is chosen to match the width of the Compton profile. As may be proved by direct integration [29], this series is the Radon transform of

$$n(\boldsymbol{q}) = \pi^{3/2} \mathrm{e}^{-(q/y_0)^2} \sum_{nlm} B_{nlm} (q/y_0)^l L_n^{l+1/2}(q^2/y_0^2) Y_{lm}(\hat{\boldsymbol{q}}) \tag{33}$$

where

$$B_{nlm} = (-1)^n 2^{2n+l} n! A_{nlm}. \tag{34}$$

Here H and L are Hermite and Laguerre polynomials, with the standard normalization [65] that the coefficient of x^m in $H_m(x)$ is 2^n, and the coefficient of x^m in $L_m^{\alpha}(x)$ is $(-1)^n/n!$. The method is thus to determine the $\{A\}$-coefficients from the data, to generate the $\{B\}$-coefficients using equation (34), and finally to obtain the reconstructed momentum distribution in the series form in equation (33).

Two properties of this inversion method make it particularly suitable for application in neutron Compton scattering. The first is that instrumental resolution is readily accounted for by including the resolution function in the fitting process used to extract the A-coefficients. In other words, the functions actually used to fit the data are the convolutions of those on the right-hand side of equation (32) with the instrumental broadening function. The second desirable property is that the expansion functions are very well matched to the characteristics of the data. Indeed, if the underlying binding potential is isotropic and harmonic, then $J(\hat{\boldsymbol{Q}}, y)$ is an isotropic Gaussian and only the first term, proportional to A_{000}, is needed. Even for anharmonic potentials, the Compton profile is expected to consist of a compact peak, and a fairly small number of terms in the expansion should suffice. The $\{A\}$-coefficients, therefore, are an economical description of the data, and the coefficients with $n > 0$ are directly related to the anharmonicity in the system [29].

The expansion of the Compton profile in equation (32) has a definite symmetry. The Hermite polynomial and the spherical harmonic each have parity $(-1)^l$, and hence $J(-\hat{\boldsymbol{Q}}, -y) = J(\hat{\boldsymbol{Q}}, y)$. This is a symmetry which is obeyed by $J(\hat{\boldsymbol{Q}}, y)$ if the impulse approximation is valid. Measured data, of course, will deviate from perfect symmetry. The procedure of fitting the symmetric expansion will ignore the antisymmetric components in the data, i.e. it will implicitly perform a symmetrization. This has, as a bonus, the effect of removing leading-order corrections to the impulse approximation (see section 2.6). For scattering from single crystals, there are likely to be additional symmetries in the directional Compton profile arising from the point group symmetry of the lattice site of the struck atom. In this case, the additional symmetry may be taken into account by expressing the expansion in terms of lattice harmonics [29].

As a final point, we discuss scaling of the data. A uniform scale factor y_0 is already included in equation (32). Choosing y_0 to be the width of the best Gaussian fit to the Compton profile matches the expansion to the data, and is likely to minimize the number of coefficients needed. However, this simple prescription is not adequate for strongly anisotropic data, where the width of the profile is very different in different directions. Here we suggest a general procedure for anisotropic scaling.

There does not appear to be a simple relationship between the inverse Radon transforms of two functions $J(\hat{\boldsymbol{Q}}, y)$ differing by a linear coordinate transformation, i.e. it does not appear useful to apply a linear transformation to the data. Instead, we ask the reverse question of how $J(\hat{\boldsymbol{Q}}, y)$ changes when we transform the momentum distribution. Let us suppose, then, that the anisotropic distribution $n(\boldsymbol{q})$ can be made reasonably isotropic by a linear scale change

$$\boldsymbol{q} \rightarrow \boldsymbol{q}' = (q_x/\alpha_x, q_y/\alpha_y, q_z/\alpha_z) \tag{35}$$

for a suitable choice of orthogonal axes xyz. Defining $n'(\boldsymbol{q}) = n(\boldsymbol{q}')$ and

$$\boldsymbol{Q}' = (\alpha_x Q_x, \alpha_y Q_y, \alpha_z Q_z) \tag{36}$$

we find the Radon transform of n' to be

$$J'(\hat{\boldsymbol{Q}}, y) \propto \int n(\boldsymbol{q}')\delta(\boldsymbol{q}' \cdot \boldsymbol{Q}' - y)\ \mathrm{d}\boldsymbol{q}' = (1/Q')J(\hat{\boldsymbol{Q}}', y/Q') \tag{37}$$

where Q' is the length of $\boldsymbol{Q}$ and $\hat{\boldsymbol{Q}}' = \boldsymbol{Q}'/Q'$, and an irrelevant constant factor has been omitted. The suggested procedure is then as follows. Given a measured Compton profile, $J(\hat{\boldsymbol{Q}}, y)$, let α_x, α_y and α_z be its characteristic widths along the chosen axes. Compute the transformed profile $J'(\hat{\boldsymbol{Q}}, y)$ according to equation (37), which amounts to a non-linear coordinate transformation. After applying the expansion technique described previously to reconstruct $n'(\boldsymbol{q})$ from J', use

$$n(\boldsymbol{q}) = n'(\alpha_x q_x, \alpha_y q_y, \alpha_z q_z) \tag{38}$$

to find the required momentum distribution corresponding to the original $J(\hat{\boldsymbol{Q}}, y)$.

The transformed Compton profile J' is roughly isotropic. For example, if $\hat{\boldsymbol{Q}}$ points along the x-axis, then $J'(\hat{\boldsymbol{Q}}, y) \propto J(\hat{\boldsymbol{Q}}, y/\alpha_x)$, which has unit width in y, by construction. Thus J' is a function for which the Radon inversion step, using the expansion method, is efficient and stable.

3.2. Anharmonic potentials

The Compton profile for scattering from a harmonically bound atom is Gaussian, and a measurement of its width yields the mean kinetic energy. Essentially the same information

might be obtainable by, for example, vibrational (infrared) spectroscopy. Where the neutron Compton scattering technique for bound atoms comes into its own, then, is in the potential to measure the anharmonicity of the binding potential, in cases where it is legitimate to treat the struck atom in terms of single-particle motion in an effective potential. It is the only technique capable of measuring Born–Oppenheimer potentials directly.

The extraction of the potential from the momentum distribution is simply a matter of inverting the Schrödinger equation:

$$V(\boldsymbol{R}) - E = (\bar{h}^2/2M)\psi^{-1}\nabla^2\psi \tag{39}$$

where $\psi(\boldsymbol{R})$ and $\psi(\boldsymbol{q})$ are Fourier transforms of each other, and the latter is obtained from $n(\boldsymbol{q}) = |\psi(\boldsymbol{q})|^2$. The phase ambiguity in extracting the momentum-space wave function from $n(\boldsymbol{q})$ is not a problem for inversion-symmetric potentials, since $\psi(\boldsymbol{q})$ can always be chosen to be real.

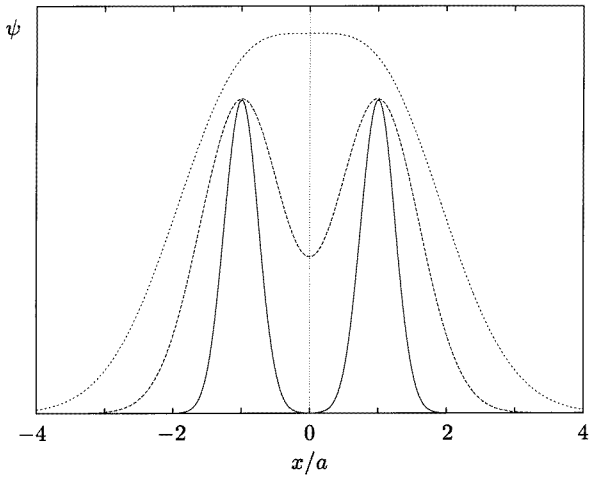

Figure 3. Model wave functions for an atom in a double-well potential. Each is the sum of two Gaussian components of width σ, centred a distance $2a$ apart. Solid line: $a/\sigma = 0.25$; dashed line: $a/\sigma = 0.6$; dotted line: $a/\sigma = 1$.

It should be noted that the technique, at least in its simplest form, is restricted to systems in which all atoms of the species under study have identical chemical environments. If they do not, the Compton profile will be a superposition of contributions from different environments.

An extreme case of an anharmonic potential is one with two minima, such as might be expected for a proton in a hydrogen bond [28, 29]. A useful model for illustrating the results expected for a double-well potential is to assume a ground state consisting of two shifted Gaussians of equal amplitude:

$$\psi(x) = \mathrm{e}^{-(x-a)^2/2\sigma^2} + \mathrm{e}^{-(x+a)^2/2\sigma^2} \tag{40}$$

in one dimension [28, 29, 66]. This function is plotted in figure 3 for selected values of the ratio a/σ, and the corresponding potentials $V(x)-E$ appear in figure 4. For the largest value of a/σ the potential consists of rather isolated harmonic wells, which gradually merge as a/σ is reduced. For $a < \sigma$, the potential is more accurately described as a single harmonic well with a shallow 'bump' in the centre, and the wave function is a single non-Gaussian peak.

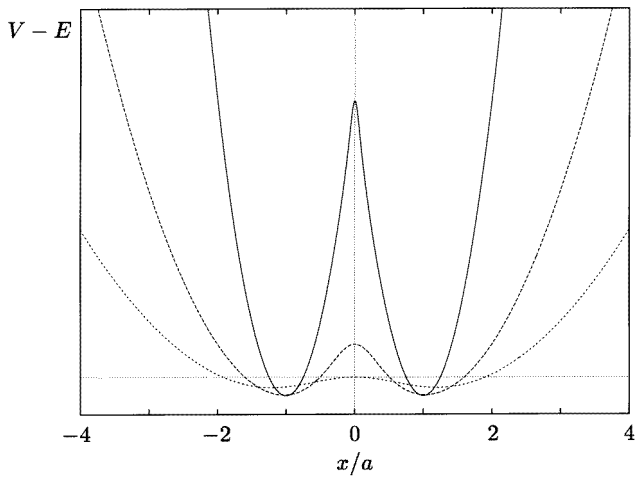

Figure 4. Model potentials $V(x) - E$ for each of the model wave functions in figure 3.

The Compton profile, $J(y) = \mathrm{e}^{-\sigma^2 y^2} \cos^2 ay$, is plotted in figure 5 for an intermediate value $a/\sigma = 0.6$. It includes an oscillatory factor, representing interference between wave functions localized in the two wells, and the overall shape is far from Gaussian. The number of oscillations in each half-width of the Gaussian envelope is roughly a/σ, so for weak anisotropy ($a/\sigma < 1$) the deviations from Gaussian form are less pronounced. The coefficients in the Hermite expansion, equation (32), corresponding to this $J(y)$ are $A_n \propto (-a^2/4\sigma^2)^n/(2n)!$, which fall off rapidly even for intermediate a/σ. In the limit of large a/σ, the oscillations are so rapid that one observes only the average, which is Gaussian as one would expect for isolated harmonic well.

This simple model may be extended to the case where the double-well potential, as in a typical hydrogen bond, is not symmetric. It is found that the asymmetry suppresses somewhat the oscillatory component in the wings of the Compton profile, which no longer goes to zero at its minima.

4. Discussion

The Compton profile in figure 5, corresponding to a model of an atom in a double-well potential, is far from Gaussian, which strongly suggests that anharmonicity of this kind should be experimentally measurable. Reiter [28, 29] has carried out an analysis of the practical limitations on measurements of anharmonicity, including the effect of sampling noise (but not of non-zero instrumental resolution), concluding that extracting meaningful atomic potential energy functions, using the series expansion method to analyse data, is feasible. On the other hand, Sivia and Silver [67], in an analysis based on Bayesian probability theory, have shown that the reconstruction of the momentum distribution from the Compton profile is an intrinsically ill-posed problem, at least for studies of the condensate fraction in superfluid helium. A simple statement of the essence of their result is that widely different momentum distributions can yield the same Compton profile within experimental error. This does not, of course, imply that momentum distributions cannot be extracted. There are grounds to believe that the inverse problem for strongly anisotropic data for

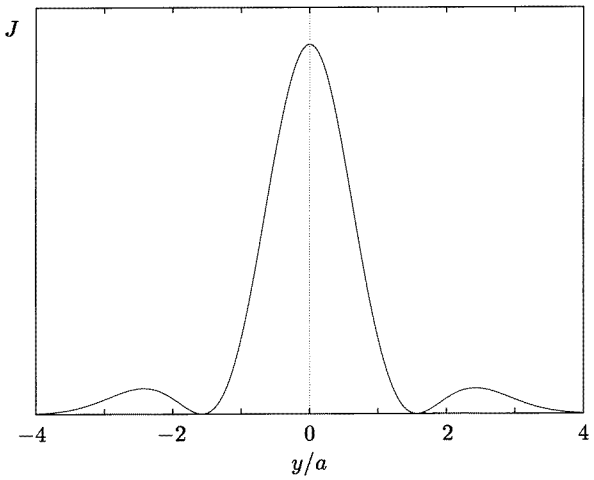

Figure 5. The Compton profile corresponding to the two-Gaussian model wave function, with $a/\sigma = 0.6$.

single crystals is better behaved than for liquid ^{4}He: if the atomic motion is approximately decoupled into independent motion along three different axes, the resulting one-dimensional inversions are more stable than the three-dimensional inversion for isotropic data. Clearly, further study of the reconstruction problem for neutron Compton scattering from solids is desirable, to establish, for example, which features of the Compton profile are most sensitive to anharmonicity, the limits to accuracy of reconstruction, and optimum algorithms.

Another question that deserves further investigation is the inclusion of corrections to the impulse approximation in the reconstruction procedure. This is a well-studied problem for scattering from superfluid helium [11], while for solids it is argued, as in section 3.1, that the corrections are negligible. Nevertheless, we note that in figure 5 it would appear to be the tails of the profile which are most sensitive to the presence of anharmonicity in the potential, and even if corrections to the impulse approximation are small relative to the recoil peak amplitude, they may be significant in the tails.

The past achievements of the neutron Compton scattering technique are impressive, ranging from the mature body of work on superfluid helium, to more recent applications in studies of quantum and classical liquids, and kinetic energies, anisotropy and quantum effects in solids. Here we have summarized the theoretical background, and the prospects for a new development of the technique, the reconstruction of momentum distributions by direct inversion from the Compton profile. Taking into account theoretical work to date, there are grounds for being cautiously optimistic. We await the first direct experimental measurement of a three-dimensional atomic potential energy function in a solid.

Acknowledgments

I would like to thank M Celli, A L Fielding, S W Lovesey, J Mayers, A S Rinat, P Schofield and D S Sivia for very helpful discussions.

References

[1] Silver R N and Sokol P E (ed) 1989 *Momentum Distributions* (New York: Plenum)
[2] Williams B (ed) 1977 *Compton Scattering* (New York: McGraw-Hill)
[3] Cooper M J 1985 *Rep. Prog. Phys.* **48** 415
[4] Kane P P 1992 *Phys. Rep.* **218** 67
[5] Antonov A N, Hodgson P E and Petkov I Zh 1988 *Nucleon Momentum and Density Distributions in Nuclei* (Oxford: Oxford University Press)
[6] Sick I 1989 *Momentum Distributions* ed R N Silver and P E Sokol (New York: Plenum) p 175
[7] Taylor R E 1991 *Rev. Mod. Phys.* **63** 573
[8] Kendall H W 1991 *Rev. Mod. Phys.* **63** 597
[9] Friedman J I 1991 *Rev. Mod. Phys.* **63** 615
[10] Hohenberg P C and Platzman P M 1996 *Phys. Rev.* **152** 198
[11] Sosnick T R, Snow W M, Silver R N and Sokol P E 1991 *Phys. Rev.* B **43** 216
[12] Glyde H R 1994 *Excitations in Solid and Liquid Helium* (Oxford: Oxford University Press)
[13] Peek D A and Simmons R O 1991 *J. Chem. Phys.* **94** 3169
[14] Fradkin M A, Zeng S-X and Simmons R O 1994 *Phys. Rev.* B **49** 3197
[15] Fradkin M A, Zeng S-X and Simmons R O 1994 *Phys. Rev.* B **49** 15 563
[16] Azuah R T, Stirling W G, Glyde H R, Sokol P E and Bennington S M 1995 *Phys. Rev.* B **51** 605
[17] Evans A C, Mayers J and Timms D N 1994 *J. Phys.: Condens. Matter* **6** 4197
[18] Fulton S, Cowley R A and Evans A C 1994 *J. Phys.: Condens. Matter* **6** 2977
[19] Andersen K H, Stirling W G, Glyde H R, Azuah R T, Bennington S M and Taylor A D 1994 *Physica* B **197** 198
[20] Andreani C, Filabozzi A, Nardone M, Ricci F P and Mayers J 1994 *Phys. Rev.* B **50** 12 744
[21] Bafile U, Zoppi M, Barocchi F, Magli R and Mayers J 1995 *Phys. Rev. Lett.* **75** 1957
[22] Azuah R T, Stirling W G, Guckelsberger K, Scherm R, Glyde H R, Bennington S M and Taylor A D 1995 *Physica* B **213+214** 454
[23] Wang Y and Sokol P E 1994 *Phys. Rev. Lett.* **72** 1040
[24] Mayers J 1993 *Phys. Rev. Lett.* **71** 1553
[25] Andreani C, Filabozzi A and Pace E 1995 *Phys. Rev.* B **51** 8854
[26] Bafile U, Zoppi M, Celli M, Magli R, Evans A C and Mayers J 1996 *Physica* B **217** 50
[27] Bafile U, Celli M and Zoppi M 1996 *Physica* B at press
[28] Reiter G and Silver R 1985 *Phys. Rev. Lett.* **54** 1047
[29] Reiter G F 1989 *Momentum Distributions* ed R N Silver and P E Sokol (New York: Plenum) p 221
[30] Sokol P E 1994 *Physics World* **7** (3) 25
[31] Lovesey S W 1994 *Neutron Scattering from Hydrogen in Materials* ed A Furrer (Singapore: World Scientific) p 19
[32] Lovesey S W 1987 *Theory of Neutron Scattering from Condensed Matter* 3rd edn, vol 1 (Oxford: Oxford University Press)
[33] Reiter G and Becher T 1985 *Phys. Rev.* B **32** 4492
[34] Dattagupta S and Reiter G F 1985 *Phys. Rev.* B **31** 1034
[35] Egelstaff P A and Schofield P 1962 *Nucl. Sci. Eng.* **12** 260
[36] Gunn J M F, Andreani C and Mayers J 1986 *J. Phys. C.: Solid State Phys.* **19** L835
[37] Mayers J 1990 *Phys. Rev.* B **41** 41
[38] Schiff L I 1968 *Quantum Mechanics* 3rd edn (New York: McGraw-Hill)
[39] Gunn J M F and Warner M 1984 *Z. Phys.* B **56** 13
[40] Mayers J, Andreani C and Baciocco G 1989 *Phys. Rev.* B **39** 2022
[41] Evans A C, Timms D N, Mayers J and Bennington S M 1996 *Phys. Rev.* B **53** 3023
[42] Fielding A L, Timms D N, Evans A C and Mayers J 1996 *J. Phys.: Condens. Matter* submitted
[43] Kittel C 1986 *Introduction to Solid State Physics* (New York: Wiley)
[44] Warner M, Lovesey S W and Smith J 1983 *Z. Phys.* B **51** 109
[45] Postorino P, Fillaux F, Mayers J, Tomkinson J and Holt R S 1991 *J. Chem. Phys.* **94** 4411
[46] Gersch H A, Rodriguez L J and Smith P N 1972 *Phys. Rev.* A **5** 1547
[47] Gersch H A and Rodriguez L J 1973 *Phys. Rev.* A **8** 905
[48] Weinstein J J and Negele J W 1982 *Phys. Rev. Lett.* **49** 1016
[49] Sears V F 1984 *Phys. Rev.* B **30** 44
[50] Kirkpatrick T R 1984 *Phys. Rev.* B **30** 1266
[51] Platzman P M and Tzoar N 1984 *Phys. Rev.* B **30** 6397

[52] Silver R N and Reiter G 1987 *Phys. Rev.* B **35** 3647
[53] Rinat A S 1987 *Phys. Rev.* B **36** 5171
[54] Silver R N 1988 *Phys. Rev.* B **37** 3794
[55] Silver R N 1988 *Phys. Rev.* B **38** 2283
[56] Silver R N 1989 *Phys. Rev.* B **39** 4022
[57] Snow W M, Wang Y and Sokol P E 1992 *Europhys. Lett.* **19** 403
[58] Stringari S 1987 *Phys. Rev.* B **35** 2038
[59] Glyde H R 1994 *Phys. Rev.* B **50** 6726
[60] Deans S R 1983 *The Radon Transform and Some of Its Applications* (New York: Wiley–Interscience)
[61] Natterer F 1986 *The Mathematics of Computerized Tomography* (Chichester: Wiley)
[62] Holschneider M 1995 *Wavelets: An Analysis Tool* (Oxford: Oxford University Press) p 392
[63] Davison M E and Grunbaum F A 1981 *Comment. Pure Appl. Math.* **34** 77
[64] Davison M E 1981 *Num. Funct. Anal. Optimiz.* **3** 321
[65] Abramowitz M and Stegun I A (ed) 1965 *Handbook of Mathematical Functions* (New York: Dover)
[66] Mayers J 1994 unpublished
[67] Sivia D S and Silver R N 1989 *Momentum Distributions* ed R N Silver and P E Sokol (New York: Plenum) p 377